

Interactions in 1-Propanol–(1,2- and 1,3-)Propanediol–H₂O: The Effect of Hydrophobic vs Hydrophilic Moiety on the Molecular Organization of H₂O

Matthew T. Parsons[†] and Yoshikata Koga^{*,†,‡}

Department of Chemistry, The University of British Columbia, 2036 Main Mall, Vancouver, B.C., Canada V6T 1Z1, and Department of Diversity Sciences, Graduate School of Science and Technology, Chiba University, Yayoi, Inage-ku, Chiba 263-8522, Japan

Received: November 14, 2001; In Final Form: May 10, 2002

The excess partial molar enthalpy and the excess chemical potential of 1-propanol in ternary systems 1-propanol–(1,2- and 1,3-)propanediols–H₂O were determined. The enthalpic interaction function between 1-propanol molecules was evaluated. The mole fraction dependence of the 1-propanol–1-propanol interaction function was used as a probe to elucidate the effect of 1,2- and 1,3-propanediols on the molecular organization of H₂O. Together with the earlier similar works on 2-propanol and glycerol, we conclude that the hydrophobic moiety diminishes the hydrogen bond connectivity of H₂O by reducing the hydrogen bond probability of bulk H₂O, while the effect of the hydrophilic moiety is primarily to reduce the degree of fluctuation inherent in liquid H₂O.

Introduction

In our earlier studies on ternary aqueous solutions of 1-propanol (abbreviated as 1P hereinafter)–A–H₂O type, we used the thermodynamic behavior of 1P as a probe to elucidate the effect of the third component A on the molecular organization of H₂O.^{1–6} For the third component A to be urea¹ or NaCl² this methodology was very successful. It was found that urea keeps the hydrogen bond connectivity of H₂O almost intact, perhaps by hydrogen-bonding to the hydrogen bond network of H₂O. However, the degree of fluctuation inherent in liquid H₂O is reduced by the presence of urea within the network.¹ A recent simulation study on aqueous urea indicated that the addition of urea leads to “stiffening” of the short time dynamics of both urea and H₂O.⁷ The effect of NaCl, on the other hand, is that 7 to 8 molecules of H₂O are bound to NaCl and the remaining H₂O is left unaffected and remains the same as in pure H₂O.² Another recent first-principle simulation study showed that the first solvation shell of Na⁺ contains 5.2 H₂O molecules and there is no effect of Na⁺ on the orientation of H₂O molecules beyond the first hydration shell.⁸

Having met some success for A = NaCl and urea, we expanded the study for A = 2-propanol(2P),⁴ and glycerol(Gly).⁶ This was to see the effect of additional –OH groups on the C–C–C backbone. To complete the project, we report here a similar study for A = (1,2- and 1,3-)propanediols (12P and 13P). Together with the previous results for A = 2P and Gly, we have now a clearer understanding on the effects of hydrophobic and hydrophilic moieties on H₂O. As shown below, the hydrophobic moiety reduces the hydrogen bond probability and hence the hydrogen bond percolation nature. The hydrophilic part, on the other hand, reduces the degree of fluctuation in hydrogen bond strength, perhaps by locking into the hydrogen bond network of H₂O.

Methodology

We briefly review our methodology here. For a ternary system 1P–A–H₂O, we determine the excess partial molar enthalpy (and entropy) of 1P. Namely, only the amount of 1P is perturbed in the ternary system with other components kept constant and the enthalpic response of the entire system is measured. Thus, the excess partial molar enthalpy of 1P, H_{1P}^E , is written as

$$H_{1P}^E = (\partial H^E / \partial n_{1P})_{n_W, n_A, P, T} \quad (1)$$

where H^E is the excess enthalpy of the entire system and n_i stands for the amount of the i th component, $i = 1P, W(H_2O)$, or A. Experimentally we determine H_{1P}^E with the fixed ratio of n_A/n_W , or the fixed initial mole fraction of A, $x_A^0 = n_A/(n_W + n)$. We then take one more derivative of H_{1P}^E with respect to n_{1P} graphically without resorting to any fitting function. See the appendix in ref 6 for detail. As we have discussed at some length earlier,^{6,8,9} a single analytic function cannot account for H_{1P}^E data over the entire composition range. Davis et al. devised a four-segment model and fitted four different analytic functions for each segments. There are, however, some problems associated with imperfect connections at segment boundaries. Instead, we take derivatives graphically without resorting to any analytic function. As a result, we realized there are three composition regions in each of which the mixing scheme is qualitatively different from those of other regions, as will be mentioned below.

We thus evaluated the enthalpic interaction, H_{1P-1P}^E , graphically as^{9,10}

$$H_{1P-1P}^E \equiv N(\partial H_{1P}^E / \partial n_{1P}) = (1 - x_{1P})(\partial H_{1P}^E / \partial x_{1P}) \quad (2)$$

where N is the total amount, $N = n_{1P} + n_A + n_W$. As argued at some length earlier,^{9,10} H_{1P-1P}^E gives a measure of 1P–1P interaction in terms of enthalpy. Since H_{1P}^E is the actual contribution of 1P in terms of enthalpy, or the actual enthalpic situation of 1P in the entire system, H_{1P-1P}^E shows the effect

* Author to whom correspondence should be addressed. Phone: (604) 822-3491. Fax: (604) 822-2847. E-mail: koga@chem.ubc.ca.

[†] The University of British Columbia.

[‡] Chiba University.

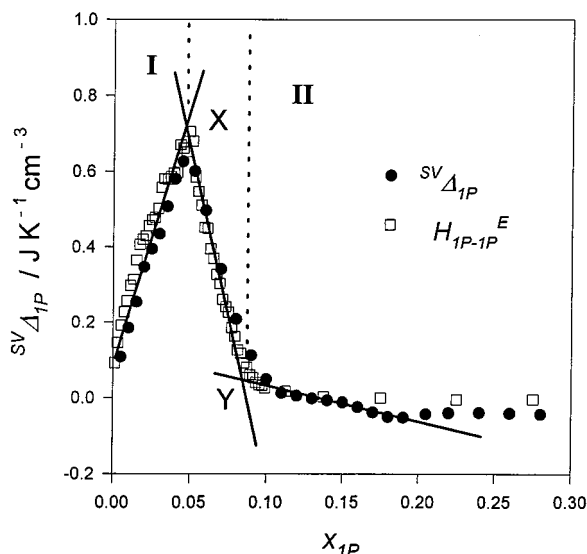


Figure 1. Enthalpic interaction function, H_{1P-1P}^E , and partial molar entropy–volume normalized fluctuation, $^{SV}\Delta_{1P}$ at 25 °C. See text.

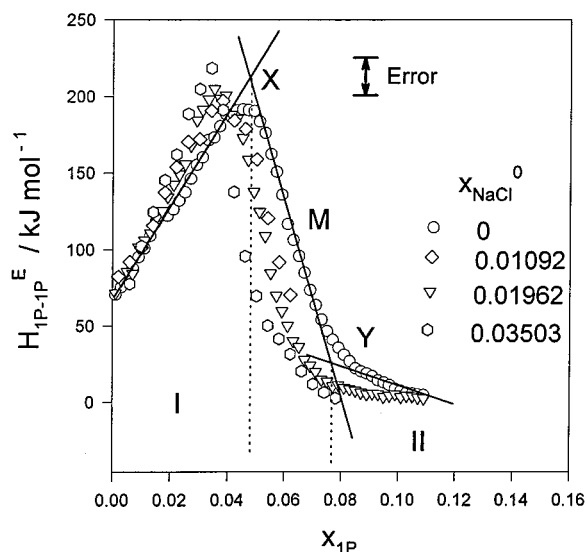


Figure 2. Enthalpic interaction function, H_{1P-1P}^E , in 1-propanol–NaCl–H₂O at 25 °C.

on the enthalpic situation of 1P when 1P is perturbed. Thus we call H_{1P-1P}^E the enthalpic interaction function.^{9,10} We emphasize that H_{1P-1P}^E is a model-free and experimentally accessible measure of the 1P–1P interaction in terms of enthalpy. The entropy analogue of eqs 1 and 2 are written as

$$S_{1P}^E = (\partial S^E / \partial n_{1P})_{n_w, n_A, p, T} \quad (3)$$

and

$$S_{1P-1P}^E \equiv N(\partial S_{1P}^E / \partial n_{1P}) = (1 - x_{1P})(\partial S_{1P}^E / \partial x_{1P}) \quad (4)$$

Rather than directly measuring S_{1P}^E , a more convenient way is to calculate S_{1P}^E as

$$TS_{1P}^E = H_{1P}^E - \mu_{1P}^E \quad (5)$$

The excess chemical potential of 1P, μ_{1P}^E , is determined by

$$\mu_{1P}^E = RT \ln\{p_{1P}/(p_{1P}^0 x_{1P})\} \quad (6)$$

where p_{1P} is the partial pressure of 1P determined in this work

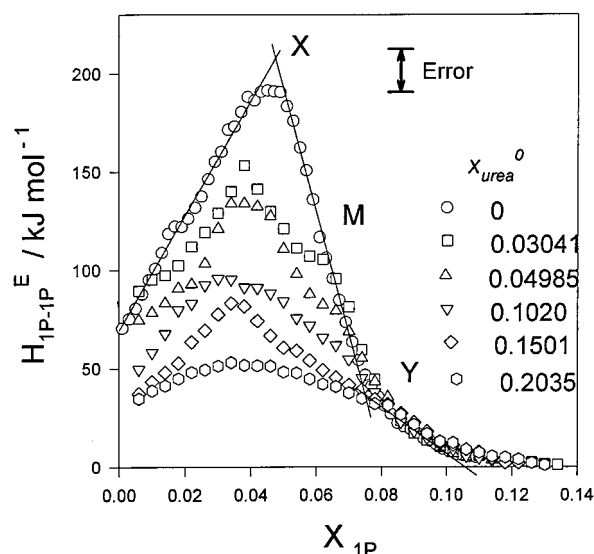


Figure 3. Enthalpic interaction function, H_{1P-1P}^E , in 1-propanol–urea–H₂O at 25 °C.

by gas analysis, or numerically calculated by the Gibbs–Duhem relation from the total pressure data.^{1,6} p_{1P}^0 is the vapor pressure of pure 1P at the same temperature. The correction for the gas-phase nonideality is negligibly small in comparison with the liquid-phase nonideality.^{9,10} Due to enthalpy–entropy compensation prevalent in aqueous solutions,¹¹ the x_{1P} -dependence of S_{1P}^E and S_{1P-1P}^E are similar to that of H_{1P}^E and H_{1P-1P}^E , particularly so in the water-rich region of our interest.

We know from previous works on binary aqueous monosols,^{9,10,12–15} that in the water-rich region what we call Mixing Scheme I is operative which is qualitatively different from mixing schemes in other regions. Mixing Scheme I is basically to protect the integrity of H₂O by enhancing the hydrogen bond network in the immediate vicinity of solute (“iceberg formation”). However, the hydrogen bond probability of bulk H₂O away from “icebergs” is progressively diminished as the solute composition increases. When the hydrogen bond probability is reduced to the hydrogen bond percolation threshold, the connectivity of the hydrogen bond network is lost, and Mixing Scheme II sets in. This effect is stronger for an alcohol with a larger hydrophobic moiety. The value of H_{AL-AL}^E is larger and the boundary between Mixing Schemes I and II occurs at a smaller value of x_{AL} , where AL stands for alcohol.

In Mixing Scheme I, it was shown that the enthalpic interaction function, H_{1P-1P}^E , for binary 1P–H₂O has the same x_{1P} -dependence as that of the partial molar entropy–volume cross fluctuation.^{14,15} Figure 1 shows the plots of $^{SV}\Delta_{1P}$ and H_{1P-1P}^E , where $^{SV}\Delta_{1P}$ is written as

$$^{SV}\Delta_{1P} \equiv N(\partial ^{SV}\Delta / \partial n_{1P}) \quad (7)$$

and

$$^{SV}\Delta \equiv \langle (\Delta S)(\Delta V) \rangle / \langle V \rangle^2 = RT\alpha_p / V \quad (8)$$

Thus, $^{SV}\Delta$ is the entropy–volume cross fluctuation normalized by the average volume of the coarse grain, $\langle V \rangle$, within which ΔS and ΔV are evaluated.^{14,15} As argued at some length earlier,^{13–15} $^{SV}\Delta$ gives a qualitative indication of the amplitude and the wavelength of the entropy–volume fluctuation. Thus, its partial molar quantity, $^{SV}\Delta_{1P}$, shows the effect of addition of 1P on $^{SV}\Delta$. Figure 1 indicates that after scaling the y-axis, both $^{SV}\Delta_{1P}$ and H_{1P-1P}^E follow exactly the same x_{1P} -dependence. We

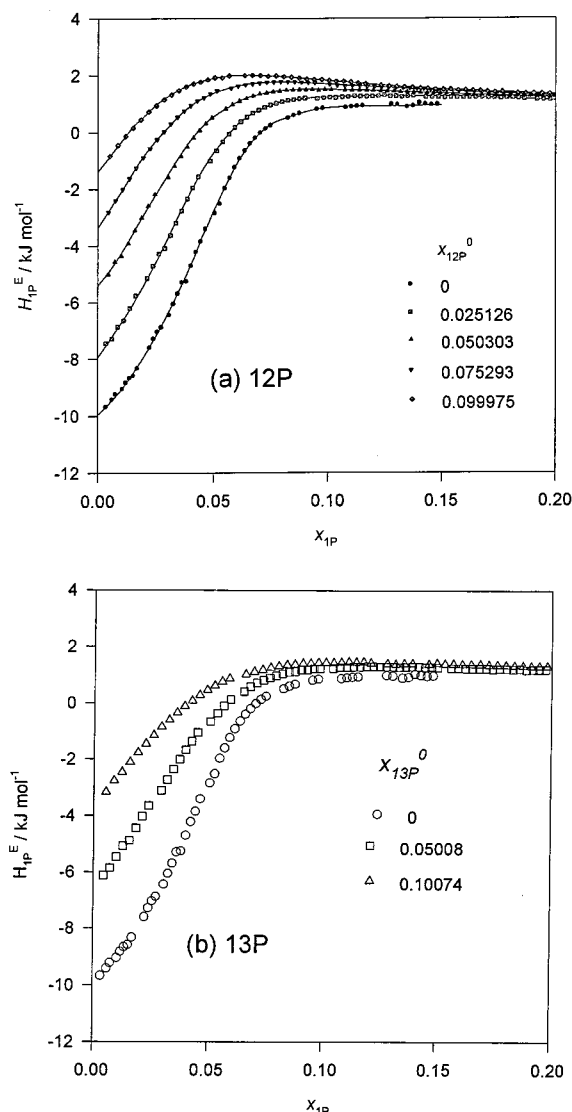


Figure 4. Excess partial molar enthalpy of 1-propanol, H_{1P}^E , (a) in 1-propanol-1,2-propanediol- H_2O , and (b) in 1-propanol-1,3-propanediol- H_2O , at 25 °C.

concluded, therefore, that $^{\text{SV}}\Delta_{1P}$ and H_{1P-1P}^E share the same cause, and that the 1P-1P interaction occurs via bulk H_2O which is characterized by the entropy-volume fluctuation.

With this knowledge, we compare the x_{1P} -dependence of H_{1P-1P}^E within Mixing Scheme I with or without a third component A. The observed difference will reflect the effect of A on the molecular organization of H_2O , since in Mixing Scheme I the integrity of H_2O is retained.

Figure 2 is the x_{1P} -dependence of H_{1P-1P}^E on addition of NaCl .² From the previous works,^{9,10,12-15} we know that the region from point X to point Y is the boundary region separating Mixing Schemes I and II. Thus, Figure 2 indicates that on addition of NaCl , the mixing scheme boundary is squeezed to a progressively smaller value of x_{1P} , while the values of H_{1P-1P}^E at $x_{1P} = 0$ and at point X remain the same within the estimated uncertainty, $\pm 10 \text{ kJ mol}^{-1}$. From the proportionality of the decrease in x_{1P} at the boundary, we concluded that a molecule of NaCl binds to the total of 7 to 8 molecules of H_2O , most likely in the form of hydrated ion pair,²⁴ rendering them unavailable for 1P to interact. From the fact that the value of H_{1P-1P}^E remains the same at $x_{1P} = 0$ and at point X, we suggested that the bulk H_2O away from the bound H_2O to NaCl is unaffected. Figure 3 shows the same plots for 1P-urea-

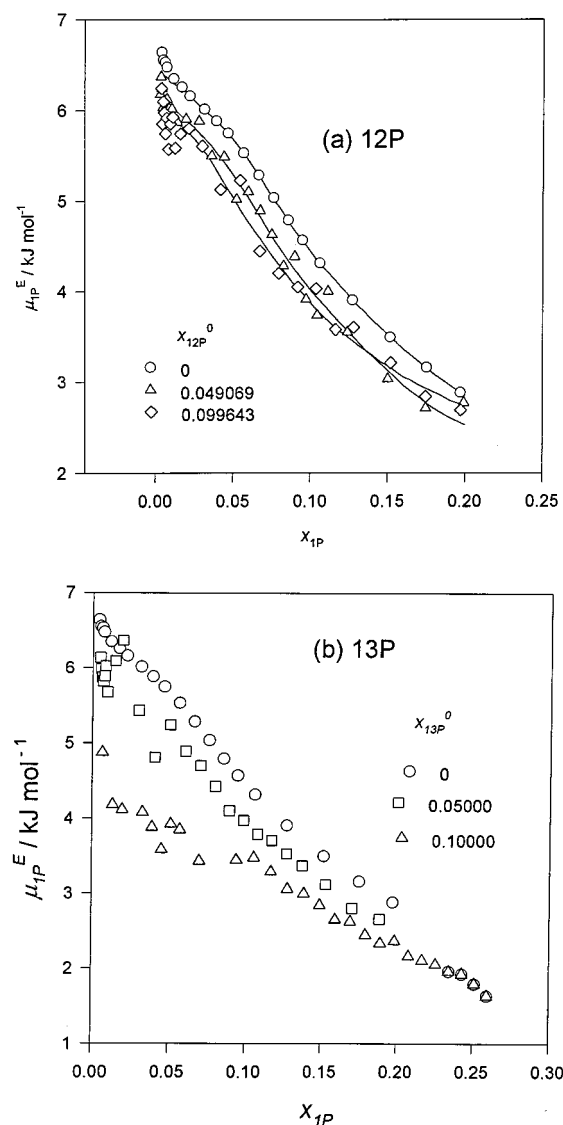


Figure 5. Excess chemical potential of 1-propanol, μ_{1P}^E , (a) in 1-propanol-1,2-propanediol- H_2O , and (b) in 1-propanol-1,3-propanediol- H_2O , at 25 °C.

H_2O . This result indicates that addition of urea does not affect the locus of the boundary much but reduces the value of H_{1P-1P}^E . Thus, we concluded that urea keeps the hydrogen bond connectivity intact, but kills the degree of fluctuation inherent to liquid H_2O .

Experimental Section

1-Propanol (ACROS, 99.5+%), 1,2-propanediol (Aldrich, 99%), and 1,3-propanediol (Aldrich, 98%) were used as supplied. They are stored over molecular sieve 3A (Aldrich) and handled in a dry nitrogen atmosphere. H_2O was distilled three times; last twice in a glass still immediately before use.

Excess partial molar enthalpies, H_{1P}^E , were determined by a homemade titration calorimeter of a design similar to that of an LKB Bromma 8700 calorimeter.¹⁶ The uncertainty in H_{1P}^E is estimated as $\pm 0.05 \text{ kJ mol}^{-1}$. Vapor pressures were measured by a static method.¹⁷ In addition, a small portion of the equilibrium gas phase was sent to a gas chromatograph for composition analysis, assuming that the partial pressures of (1,2- and 1,3-)propanediols are negligibly small. The uncertainty in the GC determination is a few percent. This translates to the uncertainty in μ_{1P}^E to be $\pm 0.3 \text{ kJ mol}^{-1}$.

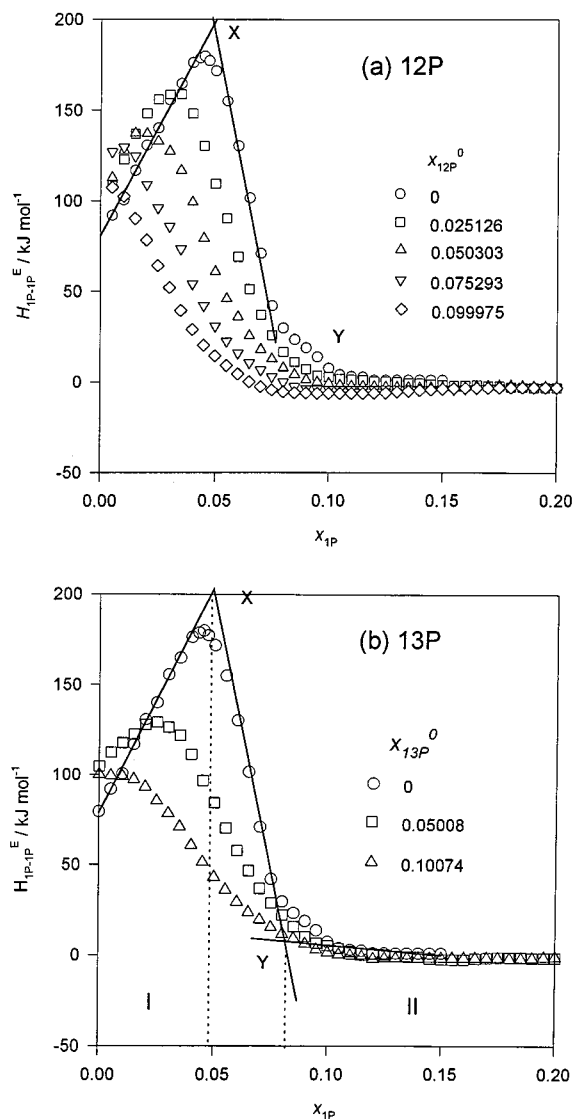


Figure 6. 1-Propanol–1-propanol enthalpic interaction function, H_{1P-1P}^E , (a) in 1-propanol–1,2-propanediol–H₂O, and (b) in 1-propanol–1,3-propanediol–H₂O, at 25 °C.

Results and Discussion

In Figure 4 H_{1P}^E data are plotted for ternary systems 1P–12P–H₂O (Figure 4a) and 1P–13P–H₂O (Figure 4b). The uncertainty is less than $\pm 0.05 \text{ kJ mol}^{-1}$. Figure 5 shows the plots of μ_{1P}^E . By comparing Figures 4 and 5, it is evident that a sharp change in H_{1P}^E up to $x_{1P} = 0.07$ followed by almost constant values of H_{1P}^E does not show up in μ_{1P}^E data. μ_{1P}^E gradually decreases to about $x_{1P} = 0.2$. Furthermore, the effect of additional 12P or 13P is also several times less conspicuous for μ_{1P}^E than that for H_{1P}^E . This is a manifestation of the entropy–enthalpy compensation prevalent in aqueous solutions.¹¹ Thus the detail of the x_{1P} -dependence of TS_{1P}^E is practically the same as that of H_{1P}^E . Since the uncertainty in μ_{1P}^E is $\pm 0.3 \text{ kJ mol}^{-1}$, the values of TS_{1P}^E will be reliable only to $\pm 0.3 \text{ kJ mol}^{-1}$ in comparison with that of H_{1P}^E being better than $\pm 0.05 \text{ kJ mol}^{-1}$. Further discussion will therefore be limited to the x_{1P} -dependence of H_{1P}^E , i.e., H_{1P-1P}^E . Figure 6 shows H_{1P-1P}^E data. The precision in H_{1P-1P}^E in this graph and that for 1P–Gly–H₂O⁶ are improved, about $\pm 5 \text{ kJ mol}^{-1}$, from the previous works^{1–5} due to a methodical graphical differentiation shown in the appendix of ref 6. Figures 7 and 8 are equivalent plots for 2-propanol(2P)⁴ and Glycerol (Gly),⁶ respectively.

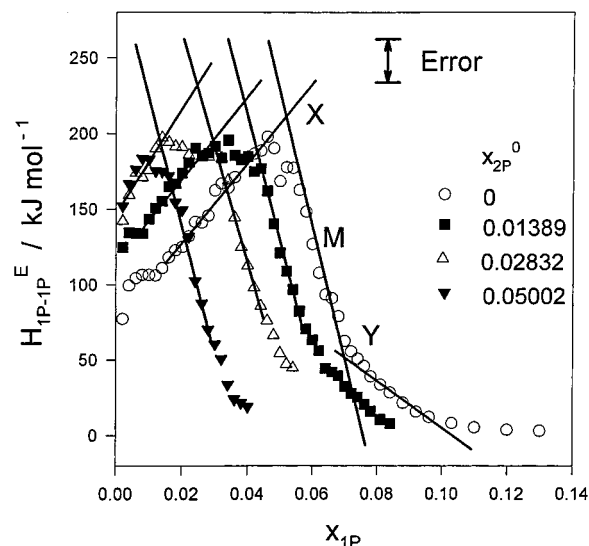


Figure 7. 1-Propanol–1-propanol enthalpic interaction function, H_{1P-1P}^E , in 1-propanol–2-propanol–H₂O at 25 °C.

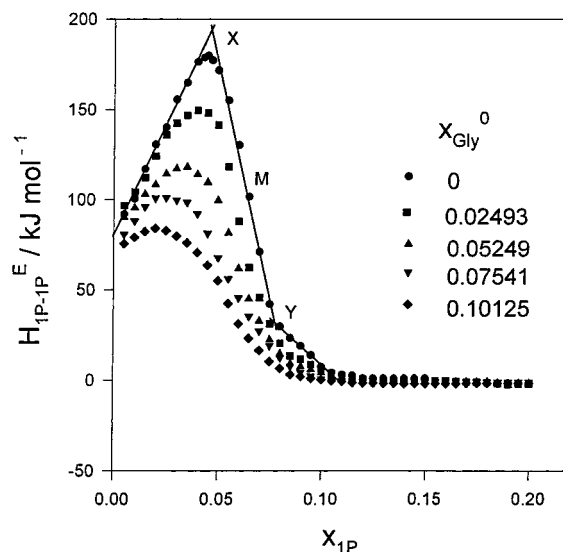


Figure 8. 1-Propanol–1-propanol enthalpic interaction function, H_{1P-1P}^E , in 1-propanol–glycerol–H₂O at 25 °C.

We know from the previous study on binary 2P–H₂O that the effect of 2P on H₂O is the same as 1P in Mixing Scheme I.¹² Thus, the presence of 2P brings about the same modification to H₂O as 1P would have done and additional 1P works the rest of the way to drive the system to Mixing Scheme II. Therefore the x_{1P} -dependence of H_{1P-1P}^E must keep its same shape but be shifted in a parallel fashion to a smaller value of x_{1P} (to the left in Figure 7) as the initial mole fraction of 2P, x_{2P}^0 , increases. This is exactly what we see in Figure 7. Or conversely, as we did in ref 4, we could conclude that 2P has the same effect on H₂O as that of 1P, from the information contained in Figure 7. The upshot is that on addition of a solute equally as hydrophobic as 1P, the profile of H_{1P-1P}^E remains the same but is shifted to the left.

We now turn to Figures 6 and 8. For 12P (Figure 6a) and 13P (Figure 6b), there is a small but definite component of shift to the left. This indicates that both do have an effect similar to that of 2P, but to a lesser extent. Namely, both have a small hydrophobic effect. Their major effects, however, are to reduce the values of H_{1P-1P}^E . This change in behavior is brought about by an additional –OH in the C–C–C backbone. Thus a hydrophilic moiety –OH serves to decrease the degree of

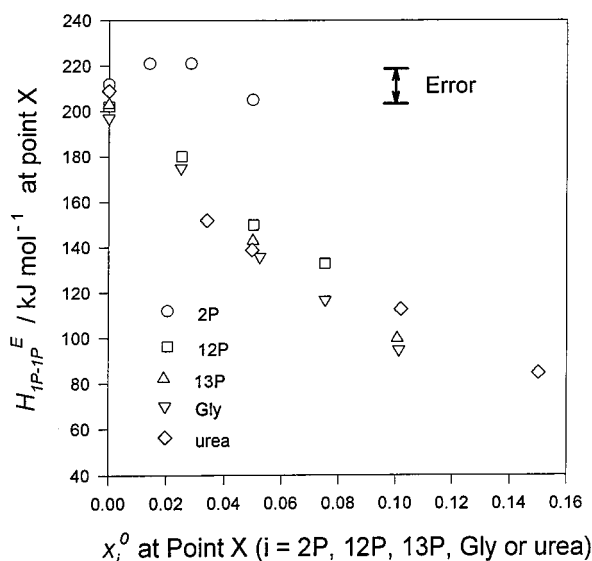


Figure 9. Values of H_{1P-1P}^E at point X. See text.

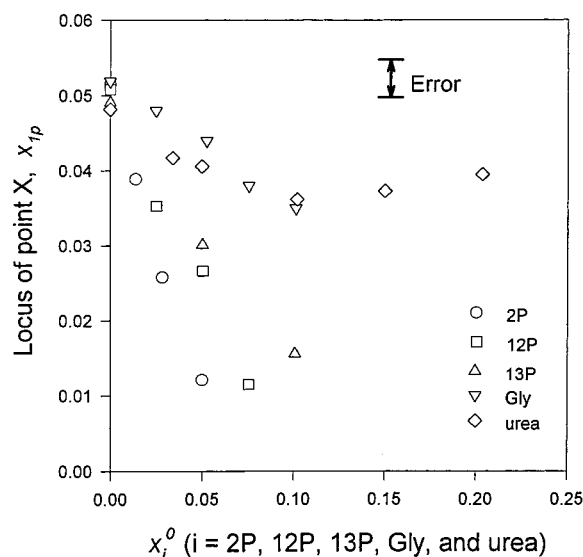


Figure 10. Loci in the mole fraction of 1-propanol of point X. See text.

fluctuation, and this occurs perhaps by participating in hydrogen bonding with H_2O network, similar to urea. We stress that this argument regarding hydrophobicity/hydrophilicity is relative only to that of 1P. Gly, on the other hand, shows primarily the effect of reducing the value of H_{1P-1P}^E , i.e., reducing the degree of fluctuation in bulk H_2O , although there is a hint of the shift to the left, Figure 8.

To see this trend more clearly we locate point X by extending linearly both sides of the peak, and plot its locus in H_{1P-1P}^E (Figure 9) and in x_{1P} (Figure 10) as a function of the initial mole fraction of the third component in question. Locating point Y has some ambiguity, and hence we limit ourselves here to the locus of point X. As seen in Figure 9, 2P does not change the values of H_{1P-1P}^E at point X. This was already discussed above. For all the others, 12P, 13P, Gly, and urea, the value of H_{1P-1P}^E decreases in the same manner as their initial mole fraction increases. This suggests that two $-OH$ or three $-OH$ on the $C-C-C$ backbone reduce the degree of fluctuation in the same way, as two $-NH_2$ and one $>C=O$ of urea. This is rather surprising, but may hint that it is the bulk part of H_2O that dictates the degree of fluctuation. Namely, the detail of how the hydrogen bond network of H_2O ends by hydrogen

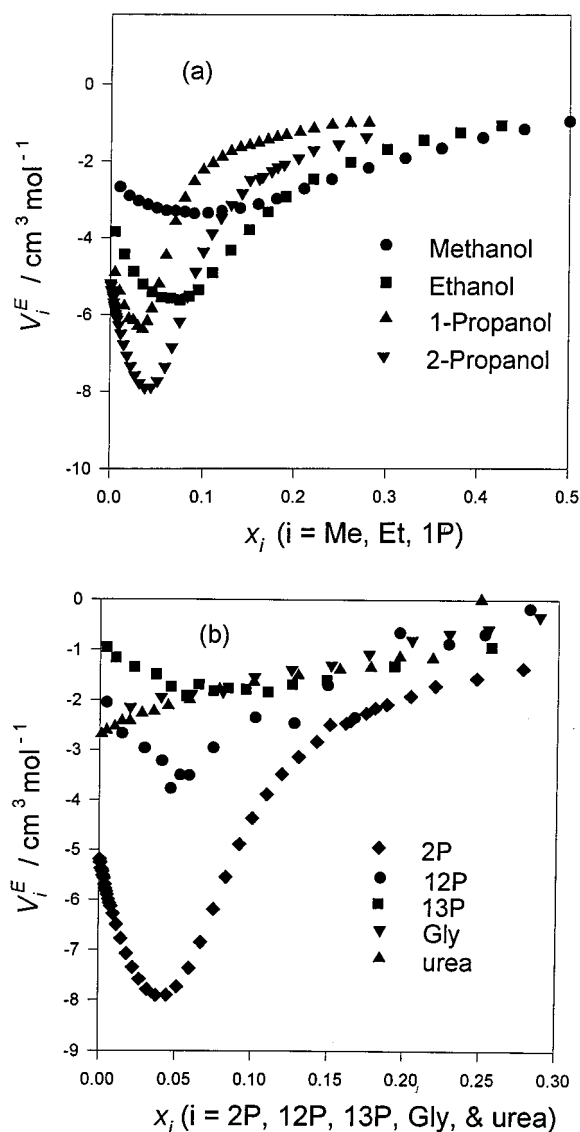


Figure 11. Excess partial molar volume of solute in respective binary aqueous solution; (a) mono-ol solutes, calculated using data in refs 18 and 19, and (b) various solutes, calculated using data in refs 20–22.

bonding to the third component is not important. On the other hand, the value of x_{1P} at point X shows a clear trend of a sharper change for a more hydrophobic moiety, Figure 10, as long as the mechanism of retarding the hydrogen bond connectivity is the same. Thus, the figure suggests that 2P, 12P, and 13P belong to this category and that the strength of hydrophobicity is in the order of $2P > 12P > 13P$. Figure 11, the excess partial molar volume, V_i^E , in the respective binary aqueous solution, shows the same trend. For an alcohol solute, V_i^E data show an initial decrease as its mole fraction increases. As argued earlier,^{9,10,12} this is due to the enhancement of the hydrogen bond network of H_2O in the immediate vicinity of a hydrophobic solute with a concomitant reduction of the hydrogen bond probability of bulk H_2O away from solutes. This “hydrophobic” signature is more conspicuous for an alcohol with a larger hydrophobic moiety, Figure 11a. From this point of view, Figure 11b indicates that 12P is weakly hydrophobic and 13P is even a weaker but still hydrophobic solute. This is consistent with the indication in Figure 10.

For Gly and urea, V_i^E data do not show a hydrophobic signature, Figure 11b. Turning back to Figure 10, we concluded in ref 1 that urea keeps the hydrogen bond connectivity intact.

Namely, the locus of x_{1P} remains the same for urea in Figure 10 within the error bar given in the figure. For Gly, on the other hand, the error bar is about a half as mentioned above, and the locus of x_{1P} shows a definite decrease, as shown in Figure 10. Thus, at least for Gly, the hydrogen bond connectivity is retarded also by the presence of Gly, primarily a hydrophilic solute. Clearly the mechanism of the retardation must be different from that of a hydrophobic moiety. However, the detail is yet to be elucidated.

In conclusion, the hydrophobic moiety in an amphiphilic alcohol is responsible for reducing the hydrogen bond probability of bulk H₂O away from the solute at the same time as it enhances the hydrogen bond network of H₂O in its immediate vicinity. As its composition increases, it eventually kills the hydrogen bond connectivity and brings about Mixing Scheme II. The hydrophilic moiety, on the other hand, participates in hydrogen bonding to the hydrogen bond network of H₂O. By so doing, it reduces the degree of fluctuation inherent in liquid H₂O. There may also be an effect of retarding the hydrogen bond connectivity by a yet unknown mechanism, at least for Gly. We stress in closing that this argument regarding the effects of the –OH group vs the C–C–C backbone is relative to what 1P does to H₂O.

Acknowledgment. We thank Eric G. M. Yee for his expert help in determining partial pressures. This research was supported by Natural Sciences and Engineering Research Council of Canada. The guest professorship awarded to Y.K. at Chiba University was financed by Project, “Strategic Centers of Excellent Education and Research”, Ministry of Education and Science, Japan. Y.K. thanks Professor K. Nishikawa and her research group for their hospitality during his stay at Chiba University.

References and Notes

- (1) To, E. C. H.; Hu, J.; Haynes, C. A.; Koga, Y. *J. Phys. Chem.* **1998**, *B102*, 10958.
- (2) Matsuo, H.; To, E. C. H.; Wong, D. C. Y.; Sawamura, S.; Taniguchi, Y.; Koga, Y. *J. Phys. Chem.* **1999**, *B103*, 2981.
- (3) To, E. C. H.; Westh, P.; Trandum, Ch.; Hvidt, Aa.; Koga, Y. *Fluid Phase Equil.* **2000**, *171*, 151.
- (4) Hu, J.; Westh, P.; Chen, D. H. C.; Haynes, C. A.; Koga, Y. *Bull. Chem. Soc. Jpn.* **2001**, *74*, 809.
- (5) Chen, D. H. C.; Liu, A. P. C.; Koga, Y. *Fluid Phase Equil.* **2001**, *189*, 31.
- (6) Parsons, M. T.; Westh, P.; Davies, J. V.; Trandum, Ch.; To, E. C. H.; Chiang, W. M.; Yee, E. G. M.; Koga, Y. *J. Solution Chem.* **2001**, *30*, 1007.
- (7) Idrissi, A.; Sokolic, F.; Perera, A. *J. Chem. Phys.* **2000**, *112*, 9479.
- (8) White, J. A.; Schwegler, E.; Galli, G.; Gygi, F. *J. Chem. Phys.* **2000**, *113*, 4668.
- (9) Koga, Y. *J. Crystallograph. Soc. Jpn.* **1995**, *37*, 172.
- (10) Koga, Y. *J. Phys. Chem.* **1996**, *100*, 5172.
- (11) Lumry, R.; Rejinder, S. *Biopolymers* **1970**, *9*, 1125.
- (12) Tanaka, S. H.; Yoshihara, H. I.; Ho, A. W.-C.; Lau, F. W.; Westh, P.; Koga, Y. *Can. J. Chem.* **1996**, *74*, 713.
- (13) Tamura, K.; Osakai, A.; Koga, Y. *Phys. Chem. Chem. Phys.* **1999**, *1*, 121.
- (14) Koga, Y. *Can. J. Chem.* **1999**, *77*, 2039.
- (15) Koga, Y.; Tamura, K. *Netsusokutei (J. Calorim. Therm. Anal., Japan)* **2000**, *27*, 195.
- (16) Koga, Y. *Can. J. Chem.* **1988**, *66*, 1187.
- (17) Koga, Y. *J. Phys. Chem.* **1991**, *95*, 4119.
- (18) Benson, G. C.; Kiyohara, O. *J. Solution Chem.* **1980**, *9*, 791.
- (19) Sakurai, M. *J. Solution Chem.* **1988**, *17*, 267.
- (20) Nakanishi, K.; Kato, N.; Maruyama, M. *J. Phys. Chem.* **1967**, *71*, 814.
- (21) Boje, L.; Hvidt, Aa. *J. Chem. Thermodyn.* **1971**, *3*, 663.
- (22) To, E. C. H.; Davies, J. V.; Tucker, M.; Westh, P.; Trandum, Ch.; Suh, K. S. H.; Koga, Y. *J. Solution Chem.* **1999**, *28*, 1137.
- (23) Davis, M. I.; Molina, M. C.; Douheret, G. *Thermochim. Acta* **1988**, *131*, 153.
- (24) Kovalenko, A.; Hirata, F. *J. Chem. Phys.* **2000**, *112*, 10403.